

This discussion paper is/has been under review for the journal Atmospheric Chemistry and Physics (ACP). Please refer to the corresponding final paper in ACP if available.

Does acetone react with HO₂ in the upper-troposphere?

T. J. Dillon¹, A. Pozzer², J. N. Crowley¹, and J. Lelieveld^{1,2}

¹Max-Planck-Institute für Chemie, Atmospheric Chemistry Division, Mainz, Germany

²EEWRC, Cyprus Institute, Nicosia, Cyprus

Received: 14 June 2010 – Accepted: 14 June 2010 – Published: 5 July 2010

Correspondence to: T. J. Dillon (terry.dillon@mpic.de)

Published by Copernicus Publications on behalf of the European Geosciences Union.

Does acetone react with HO₂ in the upper-troposphere?

T. J. Dillon et al.

Title Page

Abstract

Introduction

Conclusions

References

Tables

Figures

◀

▶

◀

▶

Back

Close

Full Screen / Esc

Printer-friendly Version

Interactive Discussion



Abstract

Recent theoretical calculations showed that reaction of HO₂ with acetone (CH₃C(O)CH₃) could be a potentially important sink for acetone and source for acetic acid in cold parts of the atmosphere (e.g. the tropopause region). The reaction HO₂+CH₃C(O)CH₃⇌(CH₃)₂C(OH)OO (R1, R-1) was therefore studied experimentally at low-temperatures for the first time. HO₂ was generated by pulsed laser photolysis, and converted by reaction with NO to OH for detection by laser induced fluorescence. Reduced yields of OH at $T < 220$ K provided evidence for stabilisation of (CH₃)₂C(OH)OO at such temperatures. In contrast, no evidence for (R1) was observed at $T > 230$ K, probably due to rapid thermal dissociation of the peroxy radical product back to reactants (R-1). The experimental data indicate that the rate coefficient for the forward reaction, $k_1(207\text{ K})$, is larger than $1.6 \times 10^{-12} \text{ cm}^3 \text{ molecule}^{-1} \text{ s}^{-1}$, in line with recent quantum mechanical calculations. In contrast, an upper limit for the equilibrium constant $K_1(T) = k_1(T)/k_{-1}(T)$ of $7.8 \times 10^{-28} \exp(50.6 \text{ kJ mol}^{-1}/RT)$ was obtained, considerably smaller than calculated from theory. Incorporation of these results into a global 3-D chemical model demonstrated that (R1) is neither a significant loss process for CH₃C(O)CH₃ nor a significant source of acetic acid in the atmosphere.

1 Introduction

Acetone, CH₃C(O)CH₃, is emitted by vegetation, biomass burning, the oceans and industry at $\sim 95 \text{ Tg yr}^{-1}$ (Jacob et al., 2002). The long lifetime of CH₃C(O)CH₃ near the surface allows for transport out of the boundary layer (Atkinson and Arey, 2003). In the cold, dry conditions of the upper troposphere (UT), CH₃C(O)CH₃ photolysis is an important initiator of free-radical chemistry, leading to generation of O₃ and OH, the primary oxidant in the troposphere (Arnold et al., 1986, 2005; Singh et al., 1995; McKeen et al., 1997; Wennberg et al., 1998). It was recently proposed (Hermans et

Does acetone react with HO₂ in the upper-troposphere?

T. J. Dillon et al.

Title Page

Abstract

Introduction

Conclusions

References

Tables

Figures

◀

▶

◀

▶

Back

Close

Full Screen / Esc

Printer-friendly Version

Interactive Discussion



al., 2004) that reaction with HO₂ (R1) initiates degradation of CH₃C(O)CH₃ in the UT.



Using quantum-chemical and statistical rate calculations, Hermans et al. (2004) studied the (R1, R-1) equilibrium, and derived an association rate coefficient $k_1(200\text{--}600\text{ K}) = 5.1 \times 10^{-15} \exp(11100/RT) \text{ cm}^3 \text{ molecule}^{-1} \text{ s}^{-1}$. The proposed product of (R1) was a weakly-bound peroxy radical, (CH₃)₂C(OH)OO, formed via addition of HO₂ to the carbonyl group and concerted transfer of an H-atom. At $T \approx 298\text{ K}$ (CH₃)₂C(OH)OO was predicted to rapidly dissociate (R-1) to reactants. This dissociation process was characterised by a strong Arrhenius-like temperature dependence, resulting in an overall $K_1(T) = 7.8 \times 10^{-28} \exp(59.7 \text{ kJ mol}^{-1}/RT)$. At $T < 220\text{ K}$ (R1) was suggested to proceed rapidly ($k_1(200\text{--}220\text{ K}) \approx 3 \times 10^{-12} \text{ cm}^3 \text{ molecule}^{-1} \text{ s}^{-1}$) with formation of significant quantities of (CH₃)₂C(OH)OO as the reverse reaction is slow ($k_{-1} < 20 \text{ s}^{-1}$). In the UT (CH₃)₂C(OH)OO would react mainly with NO (R2) and to a lesser extent HO₂ and other radicals.



Using typical tropopause conditions of $T = 200\text{ K}$, $[\text{OH}] = 6 \times 10^5$, $[\text{HO}_2] = 2.5 \times 10^7$ and $[\text{NO}] = 4 \times 10^8 \text{ molecule cm}^{-3}$, Hermans et al. (2004) calculated an effective CH₃C(O)CH₃ removal rate via (R1) and (R2) of $6 \times 10^{-7} \text{ s}^{-1}$. The predicted product of (R2), (CH₃)₂C(OH)O, would decompose to yield both CH₃C(O)OH, and CH₃ radicals which are converted HO₂ and HCHO. Thus, although the reaction consumes HO₂ in the first step, the overall net result is production of HO_x from acetone degradation.

The loss of acetone via (R1–R2) was thus predicted to compete with photolysis (R3) and reaction with OH (R4).



Large uncertainties remain however, as the acetone photolysis quantum yields recently reported by Blitz et al. (2004) are considerably smaller than earlier measurements

Does acetone react with HO₂ in the upper-troposphere?

T. J. Dillon et al.

Title Page

Abstract

Introduction

Conclusions

References

Tables

Figures

⏪

⏩

◀

▶

Back

Close

Full Screen / Esc

Printer-friendly Version

Interactive Discussion



(Gierczak et al., 1998). This discrepancy is particularly large (\approx an order of magnitude) at the low temperatures of the UT. It is unclear therefore which of (R1), (R3) or (R4) is the principal process for $\text{CH}_3\text{C}(\text{O})\text{CH}_3$ degradation, and radical production at the tropopause.

5 Confidence in the calculations of Hermans et al. (2004) was enhanced when the same group (Hermans et al., 2005) subsequently demonstrated that similar calculations reproduced the experimental results for the analogous reactions of HO_2 with HCHO (Veyret et al., 1989) and CH_3CHO (Tomas et al., 2001). Significant uncertainties remain however, and Hermans et al. (2005) acknowledged that the
10 predictions for (R1) await experimental verification. Thermochemical calculations (Benson, 2001) had previously identified the stepwise addition and rearrangement mechanism of (R1), with the group additivity method used to estimate a value of $K_1(298\text{ K})=3.2\times 10^{-19}\text{ cm}^3\text{ molecule}^{-1}$, which is considerably smaller than that calculated using the parameters from Hermans et al. (2004). Subsequently, quantum-
15 chemical methods were used (Cours et al., 2007) to calculate different intermolecular geometries for the $\text{HO}_2\text{-CH}_3\text{C}(\text{O})\text{CH}_3$ complex. Whilst similar rates for (R-1) were calculated, the considerably smaller $k_1(200\text{-}298\text{ K})\approx 3\times 10^{-16}\text{ cm}^3\text{ molecule}^{-1}\text{ s}^{-1}$ reported by Cours et al. (2007) would indicate that (R1) has no atmospheric relevance. The results of all studies to date indicate that (R1) is inefficient at around $T=298\text{ K}$, in
20 agreement with the sole laboratory investigation (Gierczak and Ravishankara, 2000), which resulted in $k_1(298\text{ K})< 8\times 10^{-16}\text{ cm}^3\text{ molecule}^{-1}\text{ s}^{-1}$. The work presented in this manuscript details the first laboratory study of (R1) at low temperatures characteristic of the upper troposphere.

Does acetone react with HO_2 in the upper-troposphere?

T. J. Dillon et al.

[Title Page](#)[Abstract](#)[Introduction](#)[Conclusions](#)[References](#)[Tables](#)[Figures](#)[⏪](#)[⏩](#)[◀](#)[▶](#)[Back](#)[Close](#)[Full Screen / Esc](#)[Printer-friendly Version](#)[Interactive Discussion](#)

2 Methods

2.1 Laboratory experiments

The experiments detailed in this work used Pulsed Laser Photolysis (PLP) reaction initiation coupled to pulsed Laser Induced Fluorescence (LIF) detection of OH. The experimental set-up has been published previously (Wollenhaupt et al., 2000; Dillon et al., 2006), and is described only briefly here. Experiments were conducted in a 500 cm³ jacketed quartz reactor. Temperature was controlled by the circulation of a cryogenic fluid through the outer jacket, and monitored with a J-type thermocouple to an estimated accuracy of ±2 K. Reaction was initiated by an excimer laser operating at 351 nm (XeF). The frequency-doubled emission from a Nd:YAG pumped dye laser was used to excite the $A^2\Sigma(v=1)\leftarrow X^2\Pi(v=0), Q_{11}(1)$ transition of OH at 281.997 nm. The resulting fluorescence from OH was detected by a photomultiplier tube, which was shielded by 309 nm (interference) and BG 26 (glass cut-off) filters.

HO₂ was generated by the 351 nm photolysis of Cl₂ (R5) in the presence of CH₃OH and O₂. Laser fluences of ≈8 mJ cm⁻² were used in conjunction with [Cl₂]=1×10¹⁴ molecule cm⁻³ to generate an estimated initial chlorine atom concentration of [Cl]~5×10¹¹ molecule cm⁻³.



Other typical reagent concentrations of [CH₃OH]=5×10¹⁴ and [O₂]=4×10¹⁶ molecule cm⁻³ were chosen such that Cl was converted within 50 μs and at 97% yield to HO₂. These experiments did not employ direct HO₂ detection, but relied on its conversion to OH by the presence of NO at concentrations of (1–3)×10¹⁴ molecule cm⁻³.



Does acetone react with HO₂ in the upper-troposphere?

T. J. Dillon et al.

Title Page

Abstract

Introduction

Conclusions

References

Tables

Figures

◀

▶

◀

▶

Back

Close

Full Screen / Esc

Printer-friendly Version

Interactive Discussion



In the absence of $\text{CH}_3\text{C}(\text{O})\text{CH}_3$, the observed LIF profiles were therefore characterised by the formation of OH (R8, ≈ 1 ms) followed by its slow decay in (R9–R10).



$\text{CH}_3\text{C}(\text{O})\text{CH}_3$ was added in concentrations of up to 1.6×10^{15} molecule cm^{-3} to this photolysis mixture. The competition between $\text{CH}_3\text{C}(\text{O})\text{CH}_3$ and NO for reaction with HO_2 , and the impact upon observed yields of OH, was used to derive kinetic parameters for (R1).

5 Precursor concentrations were determined optically by absorption at $\lambda=184.9$ nm in a 43.8 cm absorption cell located downstream of the reactor (Dillon et al., 2005). Literature values for $\sigma_{185\text{nm}}(\text{CH}_3\text{C}(\text{O})\text{CH}_3)=3.01 \times 10^{-18}$ cm^2 molecule $^{-1}$ (Gierczak et al., 2003) and $\sigma_{185\text{nm}}(\text{CH}_3\text{OH})=6.65 \times 10^{-19}$ cm^2 molecule $^{-1}$ (Dillon et al., 2005) were used to determine $[\text{CH}_3\text{C}(\text{O})\text{CH}_3]$ and $[\text{CH}_3\text{OH}]$ via the Beer-Lambert law. Values of
10 $[\text{NO}]$, $[\text{Cl}_2]$, $[\text{O}_2]$ and $[\text{N}_2]$ were calculated to an estimated accuracy of $\pm 15\%$ from bulb or cylinder partial-pressures, calibrated mass-flow rates and measurements of T and P . Total gas flow rates of 500–1000 cm^3 (STP) min^{-1} ensured that a fresh gas sample was available for photolysis at each pulse.

Analysis of the experimental OH profiles was assisted by use of numerical simulation
15 using the FACSIMILE program (Curtis and Sweetenham, 1987) using an appropriate chemical scheme. The reactions considered are described in Sect. 3.

Chemicals: liquid samples of $\text{CH}_3\text{C}(\text{O})\text{CH}_3$ (Merck > 99.8%) and CH_3OH (LS Labor > 99.8%) were subject to repeated freeze-pump-thaw cycles; NO (Linde) was distilled by repeatedly removing the light boiling fractions at 77 K and discarding the
20 frozen residue as the sample warmed; N_2 and O_2 (Messer 5.0, 99.999%), and Cl_2 (Linde 2.0% in He) were used as supplied.

Does acetone react with HO_2 in the upper-troposphere?

T. J. Dillon et al.

Title Page

Abstract

Introduction

Conclusions

References

Tables

Figures

◀

▶

◀

▶

Back

Close

Full Screen / Esc

Printer-friendly Version

Interactive Discussion



2.2 Atmospheric modelling

The general circulation model for atmospheric chemistry ECHAM5/MESy1 (henceforth EMAC), (Jöckel et al., 2005, 2006) was used to investigate the atmospheric impact of the values of k_1 and K_1 derived in this work. EMAC was used with T42 spectral resolution, corresponding to $2.8^\circ \times 2.8^\circ$ at the surface. The vertical resolution was 90 layers, of which about 25 were located in the troposphere. The model dynamics was weakly nudged (Jeuken et al., 1997; Lelieveld et al., 2007) towards the analysis data of the ECMWF operational model (up to 100 hPa) in order to realistically represent the meteorology in the troposphere. Important changes were made to the model to account for recent improvements in the kinetic/photochemical database for $\text{CH}_3\text{C}(\text{O})\text{CH}_3$ and $\text{CH}_3\text{C}(\text{O})\text{OH}$. The quantum yields for $\text{CH}_3\text{C}(\text{O})\text{CH}_3$ photolysis were based on results from Blitz et al. (2004) as preferred by IUPAC (Atkinson et al., 2006). In addition, rate coefficients for $\text{CH}_3\text{C}(\text{O})\text{OH}$ formation and loss processes were updated (see Table 1) to reflect recent laboratory data on the reaction of HO_2 with acetylperoxy radicals (Hasson et al., 2004; Dillon and Crowley, 2008; Jenkin et al., 2008) and several recent studies of the $\text{OH} + \text{CH}_3\text{C}(\text{O})\text{OH}$ reaction (IUPAC, 2010)

3 Results and discussion

3.1 Laboratory studies

Evidence for reaction was only observed at the lowest temperatures. Fairly complex chemistry controlled the OH production and loss depicted in the OH profiles, so that numerical simulations (see below) were used to obtain best estimates for $k_1(T)$ and $K_1(T)$.

Does acetone react with HO_2 in the upper-troposphere?

T. J. Dillon et al.

Title Page

Abstract

Introduction

Conclusions

References

Tables

Figures

◀

▶

◀

▶

Back

Close

Full Screen / Esc

Printer-friendly Version

Interactive Discussion



3.1.1 Evidence for reaction between HO₂ and CH₃C(O)CH₃ at $T < 230$ K

In back-to-back experiments where unchanged reagent concentrations and laser fluences were used, time-resolved OH LIF profiles, were recorded prior to and following the addition of CH₃C(O)CH₃. Figure 1 displays a pair of typical profiles recorded following generation of HO₂ (R5–R7) in the presence of excess [NO]= 1.5×10^{14} molecule cm⁻³ at $T=207$ K. In the absence of CH₃C(O)CH₃ (square datapoints), OH was formed on a timescale (≈ 500 μ s) consistent with the kinetics of HO₂+NO (R8). The circles were recorded following addition of [CH₃C(O)CH₃]= 7.5×10^{14} molecule cm⁻³, and are characterised by a dramatic reduction in the OH LIF signal. Such a change in OH makes sense if CH₃C(O)CH₃ efficiently competes for the HO₂, so reducing the amount available for conversion (R8) to OH. There are however a number of physical and chemical processes by which CH₃C(O)CH₃ may perturb the LIF signal in these experiments; these must be isolated from the impact of (R1–R2) if we are to obtain a reasonable estimate for the efficiency of the HO₂–CH₃C(O)CH₃ interaction.

The effect of CH₃C(O)CH₃ upon physical processes was assessed previously (Dillon and Crowley, 2008). No changes to LIF intensity were observed following addition of CH₃C(O)CH₃ at concentrations up to 4×10^{15} molecule cm⁻³, demonstrating that changes to fluorescence yields and/or detection efficiency of OH were negligible. The changes in LIF signal observed in Fig. 1 therefore directly reflect changes to OH production and loss chemistry due to CH₃C(O)CH₃. Other parameters such as photolysis/probe laser fluence and reagent concentrations were unchanged; importantly therefore, data obtained in the absence of CH₃C(O)CH₃ may be used to calibrate the experiment.

A semi-quantitative analysis of the data presented in Fig. 1 may be made by consideration of first-order rate constants for HO₂ removal (assumed equivalent to the observed OH formation rate) and ignoring the thermal decomposition of the product peroxy radical. In the absence of CH₃C(O)CH₃, HO₂

Does acetone react with HO₂ in the upper-troposphere?

T. J. Dillon et al.

[Title Page](#)[Abstract](#)[Introduction](#)[Conclusions](#)[References](#)[Tables](#)[Figures](#)[⏪](#)[⏩](#)[◀](#)[▶](#)[Back](#)[Close](#)[Full Screen / Esc](#)[Printer-friendly Version](#)[Interactive Discussion](#)

Does acetone react with HO₂ in the upper-troposphere?

T. J. Dillon et al.

Title Page

Abstract

Introduction

Conclusions

References

Tables

Figures

◀

▶

◀

▶

Back

Close

Full Screen / Esc

Printer-friendly Version

Interactive Discussion

is removed by reaction with NO at a rate of $k_8[\text{NO}] = 2000 \text{ s}^{-1}$ (uses $k_8(200\text{--}400 \text{ K}) = 3.45 \times 10^{-12} \exp(270/T) \text{ cm}^3 \text{ molecule}^{-1} \text{ s}^{-1}$; Atkinson et al., 2004). As a first approximation we attribute all of the reduction in observed OH ($\approx 40\%$) to the impact of $\text{CH}_3\text{C}(\text{O})\text{CH}_3$ via (R1). To compete with (R8), the $\text{CH}_3\text{C}(\text{O})\text{CH}_3$ must se-
 5 quester HO_2 at a rate given by $k_1[\text{CH}_3\text{C}(\text{O})\text{CH}_3]$ of many hundreds of s^{-1} , implying that $k_1(207 \text{ K}) > 1 \times 10^{12} \text{ cm}^3 \text{ molecule}^{-1} \text{ s}^{-1}$. This value is in line with the predictions from Hermans et al. (2004), and considerably larger than that calculated by Cours et al. (2007). A series of such back-to-back experiments was conducted, and the LIF signals observed were in roughly inverse proportion to $[\text{CH}_3\text{C}(\text{O})\text{CH}_3]$, indicating that this
 10 result is robust. Details of the experimental conditions used in these and other experiments are listed in Table 2. Note that an exact analytical treatment of these datasets was not appropriate, as OH production did not commence at $t=0$ (there is a short delay whilst the precursor HO_2 is generated).

Experiments conducted at somewhat higher temperature were characterised by
 15 much smaller changes in OH. For example, Fig. 2 displays a typical pair of OH profiles obtained at $T=228 \text{ K}$, wherein the addition of $[\text{CH}_3\text{C}(\text{O})\text{CH}_3] = 1 \times 10^{15} \text{ molecule cm}^{-3}$ resulted in an approximate 15% reduction in LIF intensity. Whilst this change in OH could be due to (R1), the addition of $\text{CH}_3\text{C}(\text{O})\text{CH}_3$ to the reaction mixtures could impact on OH via other chemical processes, e.g. by removing OH directly (R4), or the
 20 precursor Cl radicals in (R11).



In summary, the observations presented in Figs. 1 and 2 provide evidence for the theoretical predictions of Hermans et al. (2004) of a significant forward rate coefficient with $k_1(200\text{--}210 \text{ K}) \approx 3 \times 10^{12} \text{ cm}^3 \text{ molecule}^{-1} \text{ s}^{-1}$ and a strongly temperature dependent
 25 reverse process (R-1). To isolate and quantify the effects on OH that were attributable to (R1), numerical simulations of the datasets were conducted.

3.1.2 Simulations to obtain k_1 and K_1 for $\text{HO}_2+\text{CH}_3\text{C}(\text{O})\text{CH}_3$

Numerical simulation of kinetic data using the FACSIMILE program (Curtis and Sweetenham, 1987) was used to assess the reactions of $\text{CH}_3\text{C}(\text{O})\text{CH}_3$ with the radicals Cl , HO_2 and OH . Experimentally determined values of P , T , $[\text{CH}_3\text{C}(\text{O})\text{CH}_3]$, $[\text{CH}_3\text{OH}]$, $[\text{NO}]$, $[\text{O}_2]$, $[\text{Cl}_2]$, together with calculated $[\text{Cl}]$ were used to initialise the simulations. Table 3 lists the reactions and rate coefficients used to simulate the kinetic behaviour of $[\text{Cl}]$, $[\text{HO}_2]$, $[\text{OH}]$ and $[(\text{CH}_3)_2\text{C}(\text{OH})\text{OO}]$. The results of one such simulation are displayed as the black, dashed line passing through the square datapoints on Fig. 1. The OH production and loss processes are reasonably well-characterised, and these datasets obtained in the absence of $\text{CH}_3\text{C}(\text{O})\text{CH}_3$ were therefore used to define the LIF sensitivity (fixing the relative positions of the LIF and $[\text{OH}]$ y -axes on Fig. 1). Simulation of the data recorded in the presence of $\text{CH}_3\text{C}(\text{O})\text{CH}_3$ (e.g. circles in Fig. 1) was less straightforward. The simulated $[\text{OH}]$ profiles were particularly sensitive to the target reaction (R1), but also sensitive to the chosen rate coefficients for the reaction of $(\text{CH}_3)_2\text{C}(\text{OH})\text{OO}$ with NO . The rate coefficients for (R8), (R4) and (R10) are very well established (IUPAC), essentially leaving three unknowns $k_1(T)$, $K_1(T)$ and $k_2(T)$ to be estimated for simulation at each experimental temperature (207–298 K).

There are no theoretical or experimental studies of (R2), $(\text{CH}_3)_2\text{C}(\text{OH})\text{OO}+\text{NO}$, in the literature. In this work, we have therefore adopted the expression $k_2(200\text{--}300\text{ K})=2.7\times 10^{-12}\exp(360/T)$, listed by Atkinson et al. (2004) for the reaction of NO with another C_3 peroxy radical, $\text{CH}_3\text{CH}(\text{O}_2)\text{CH}_3$. For the simulations presented in Fig. 1 this expression gives $k_2(207\text{ K})=1.5\times 10^{-11}\text{ cm}^3\text{ molecule}^{-1}\text{ s}^{-1}$, which as Hermans et al. (2004) noted is the value reported for a number of peroxy+ NO reactions at around $T=200\text{ K}$.

Initial values of $k_1(207\text{ K})=3.2\times 10^{-12}\text{ cm}^3\text{ molecule}^{-1}\text{ s}^{-1}$ and $K_1(207\text{ K})=9.1\times 10^{-13}\text{ cm}^3\text{ molecule}^{-1}$ were taken from the calculations of Hermans et al. (2004). The resulting simulation of the $[\text{CH}_3\text{C}(\text{O})\text{CH}_3]=7.5\times 10^{14}\text{ molecule cm}^{-3}$ data in Fig. 1 is displayed as the red, dot-dashed line. This simulation has clearly over-

Does acetone react with HO_2 in the upper-troposphere?

T. J. Dillon et al.

Title Page

Abstract

Introduction

Conclusions

References

Tables

Figures

◀

▶

◀

▶

Back

Close

Full Screen / Esc

Printer-friendly Version

Interactive Discussion



estimated the impact of $\text{CH}_3\text{C}(\text{O})\text{CH}_3$ on the observed OH (circle datapoints). Either the true value of k_1 is smaller than that calculated by Hermans et al., or the dissociation of the peroxy radical proceeds faster. Whilst it was not possible to determine both k_1 and K_1 from one dataset, a lower-limit for $k_1(207\text{ K})=1.6\times 10^{-12}\text{ cm}^3\text{ molecule}^{-1}\text{ s}^{-1}$ was obtained in simulations where the dissociation process (R-1) was neglected. A larger value of $k_1(207\text{ K})$ could of course also account for the experimental observations, if associated with faster re-dissociation (R-1) of $(\text{CH}_3)_2\text{C}(\text{OH})\text{OO}$ back to $\text{CH}_3\text{C}(\text{O})\text{CH}_3$ and HO_2 .

An experimentally determined $k_1(207\text{ K})\geq 1.6\times 10^{-12}\text{ cm}^3\text{ molecule}^{-1}\text{ s}^{-1}$ is in stark contrast to the results from Cours et al. (2007), who calculated values of $k_1(200\text{--}220\text{ K})=3.2\times 10^{-16}\text{ cm}^3\text{ molecule}^{-1}\text{ s}^{-1}$ (and $K_1(207\text{ K})=6.6\times 10^{-17}\text{ cm}^3\text{ molecule}^{-1}$). The green, dotted line on Fig. 1 displays the results of a simulation using the parameters of Cours et al., which clearly underestimate the experimentally observed effect of $\text{CH}_3\text{C}(\text{O})\text{CH}_3$ on OH (circle datapoints). Note that simulations using $k_1=0$ were indistinguishable from the green, dotted line (Cours et al., 2007). Differences in the simulations with $[\text{CH}_3\text{C}(\text{O})\text{CH}_3]=0$ (black, dashed line), and the $k_1=0$ green, dotted line were principally due to an increased OH removal rate via recombination with the added acetone (R4). Good reproduction of the experimental data was obtained by using the k_1 value from Hermans et al. (2004) and a value of $k_{-1}=2300\text{ s}^{-1}$. We can then calculate a value for the equilibrium constant of $K_1(207\text{ K})=k_1/k_{-1}=1.4\times 10^{-15}\text{ cm}^3\text{ molecule}^{-1}$.

A similar methodology was used to simulate the $T=228\text{ K}$ data displayed in Fig. 2. In contrast to results obtained at lower T , there is little difference between the data obtained at $[\text{CH}_3\text{C}(\text{O})\text{CH}_3]=0$ data (squares), and at $[\text{CH}_3\text{C}(\text{O})\text{CH}_3]=1.0\times 10^{15}\text{ molecule cm}^{-3}$ (circles). The black, dashed line again represents a simulation of the $[\text{CH}_3\text{C}(\text{O})\text{CH}_3]=0$ data, which reproduced the experimental data well and therefore was used to fix the relative positions of the LIF and $[\text{OH}]$ y -axes. The red, dot-dashed line represents a simulation of the circles data, using the values of k_1 and K_1 from Hermans et al. (2004), and again clearly overestimates the perturbation to $[\text{OH}]$ caused by $\text{CH}_3\text{C}(\text{O})\text{CH}_3$. A more reasonable reproduction of the circles was

Does acetone react with HO_2 in the upper-troposphere?

T. J. Dillon et al.

[Title Page](#)[Abstract](#)[Introduction](#)[Conclusions](#)[References](#)[Tables](#)[Figures](#)[◀](#)[▶](#)[◀](#)[▶](#)[Back](#)[Close](#)[Full Screen / Esc](#)[Printer-friendly Version](#)[Interactive Discussion](#)

obtained using $k_1=0$ (green, dotted line), or up to $4 \times 10^{-13} \text{ cm}^3 \text{ molecule}^{-1} \text{ s}^{-1}$ if (R-1) was neglected. This simulation demonstrates that within the experimental scatter, little or no interaction between HO_2 and $\text{CH}_3\text{C}(\text{O})\text{CH}_3$ is evident at $T=228 \text{ K}$. Similar results were obtained at all higher temperatures (see Table 2), in line with the only previous experimental study by (Gierczak and Ravishankara, 2000) who observed no reactive loss of HO_2 in the presence of $\text{CH}_3\text{C}(\text{O})\text{CH}_3$ at 298 K , and with the prediction of Benson (2001).

In all experiments, a large excess of $[\text{NO}] > 1 \times 10^{14} \text{ molecule cm}^{-3}$ was available to irreversibly trap (R2) the product peroxy radical, and prevent re-dissociation (R-1) to HO_2 and $\text{CH}_3\text{C}(\text{O})\text{CH}_3$. Consequently, whilst (R1) was considered important only in atmospheric conditions of $T < 220 \text{ K}$, these experiments were sensitive to (R1) over a larger range of temperatures ($< 260 \text{ K}$) if the values of k_1 and K_1 reported by Hermans et al. (2004) were accurate. We estimate that the rate of irreversible product formation was $k_2(200-230 \text{ K}) \times [\text{NO}] \approx 2000 \text{ s}^{-1}$, whilst both Hermans et al. (2004) and Cours et al. (2007) calculated a slow dissociation rate given by $k_1/K_1 \approx 4 \text{ s}^{-1}$ at $T=207 \text{ K}$, rising to $\approx 50 \text{ s}^{-1}$ at 228 K . Either k_1 itself has an unusually strong non-Arrhenius temperature dependence accounting for the lack of reaction observed at $T > 228 \text{ K}$, or the barrier to thermal dissociation (R-1) has been overestimated by theory. We consider the latter to be more likely, and therefore simulated all experimental datasets (see Table 2) using $k_1(T) = 5.1 \times 10^{-15} \exp(11100/RT) \text{ cm}^3 \text{ molecule}^{-1} \text{ s}^{-1}$ from Hermans et al. (2004), in line with our observed value of $k_1(207 \text{ K}) > 1.6 \times 10^{-12} \text{ cm}^3 \text{ molecule}^{-1} \text{ s}^{-1}$. Values of k_{-1} were varied so as to obtain the best reproduction of the experimental data. It was possible to obtain values for the equilibrium constant at five temperatures below 230 K via $K_1 = k_1/k_{-1}$; these are listed in Table 2 and displayed in van't Hoff format in Fig. 3. The error bars associated with the blue square datapoints are indicative of experimental uncertainty, i.e. calculated from the range of k_{-1} values that were consistent with the observed OH profiles. A best estimate of the reaction enthalpy was obtained from a "3rd Law" fit of the data using $K_1(T) = A \exp\{-\Delta H_1/(RT)\}$ with the pre-exponential factor constrained by the calculated reaction entropy (Hermans et

Does acetone react with HO_2 in the upper-troposphere?

T. J. Dillon et al.

Title Page

Abstract

Introduction

Conclusions

References

Tables

Figures

◀

▶

◀

▶

Back

Close

Full Screen / Esc

Printer-friendly Version

Interactive Discussion



al., 2004) to $A=7.8\times 10^{-28}\text{ cm}^3\text{ molecule}^{-1}$ to yield $\Delta H_1=(48.4\pm 0.3)\text{ kJ mol}^{-1}$. Also displayed in Fig. 3 are the results from Hermans et al. (2004) and Cours et al. (2007), and an extrapolation calculated using the values of $K_1(298\text{ K})=3.2\times 10^{-19}\text{ cm}^3\text{ molecule}^{-1}$ and $\Delta H_1=51.9\text{ kJ mol}^{-1}$ from Benson (2001).

In an investigation such as this, where numerical simulations were necessary to analyse the experimental data, there were many potential sources of error. Systematic uncertainties, both experimental and from the literature/estimated rate coefficients used for simulations almost certainly outweigh the experimental scatter depicted by the error bars in Fig. 3. The hairlines associated with the datapoints in Fig. 3 represent a generous assessment of the real systematic uncertainty in our determinations of K_1 , with important contributions from the following (2σ) uncertainties: $\pm 5\%$ in $[\text{CH}_3\text{C}(\text{O})\text{CH}_3]$; $\pm 15\%$ in $[\text{NO}]$; $\pm 2\text{ K}$ in T ; $\pm 50\%$ in k_2 ; $\pm 20\%$ in k_8 . A similarly constrained fit then yields an upper-limit to K_1 of $7.8\times 10^{-28}\text{ exp}\{50.6\text{ kJ mol}^{-1}/(RT)\}\text{ cm}^3\text{ molecule}^{-1}$.

Note that the experimental determination of ΔH_1 is independent of the particular values of k_1 used to initiate the simulations, since it is derived from K_1 (the ratio k_1/k_{-1}). We reiterate however that since a reasonably fast forward reaction was observed at 207 K, then the explanation of a barrier for (R-1) some 9 kJ mol^{-1} smaller than calculated by theory makes the most physical sense. This is outside the error estimated by Hermans et al. (2004) of $\pm 2\text{ kJ mol}^{-1}$ uncertainty for all stationary points on their potential energy surface. Results from the more recent theoretical calculations of Cours et al. (2007) also lie well outside the range of K_1 obtained from these experiments. Observations of a rapid k_1 in this work are also in stark contrast to the findings of Cours et al. (2007). There is however, reasonable agreement with the values of K_1 and ΔH_1 estimated from group additivity (Benson, 2001).

3.2 Modelling studies

The modelling focused on the role of (R1) as an $\text{CH}_3\text{C}(\text{O})\text{CH}_3$ degradation process in the UT and its potential as a source of acetic acid, $\text{CH}_3\text{C}(\text{O})\text{OH}$, as postulated by

Does acetone react with HO₂ in the upper-troposphere?

T. J. Dillon et al.

Title Page

Abstract

Introduction

Conclusions

References

Tables

Figures

◀

▶

◀

▶

Back

Close

Full Screen / Esc

Printer-friendly Version

Interactive Discussion



Hermans et al. (2004). The simulation S1, which has been extensively described and evaluated previously (Jöckel et al., 2006; Pozzer et al., 2007) was used as a point of reference. The chemical mechanism (Sander et al., 2005) was augmented by (R1), (R-1), (R2) and the reaction of HO₂ with the peroxy radical (R12), which provides
5 a additional route for removal of RO₂ (see Table 1):



A further two simulations were performed using this augmented chemical mechanism: in simulation SR1, reactions (R1) and (R-1) were excluded; whilst simulation SR2 used the full augmented mechanism including (R1) and (R-1).

10 Figure 4 displays the calculated decay rate for CH₃C(O)CH₃ at 30° N on the 21 June 2000, based on the results of simulations SR1 and SR2. The largest removal rates due to (R1) are located in the UT (where the lowest temperature conditions are found), with a maximum at around 100 hPa. If the value calculated by Hermans et al. (2004) for the equilibrium rate *K*₁ is used, (R1) contributes significantly to CH₃C(O)CH₃ removal, with
15 a similar order of magnitude to photolysis (R3) and reaction with OH (R4). If however the upper-limit for *K*₁ obtained in this work is used the removal rate due to (R1) is approximately three orders of magnitude smaller than those of (R3) or (R4). Reaction (R1) clearly has negligible impact on the global budget of CH₃C(O)CH₃.

Similarly, in terms of acetic acid formation, the contribution of (R1) was found to
20 be almost negligible compared to other sources (e.g., reaction between CH₃C(O)O₂ and HO₂) and does not help to explain observations of high acetic acid mixing ratios in the upper troposphere. In fact, updating the chemical mechanism with new kinetic data resulted in reduced production rates and enhanced loss rates of CH₃C(O)OH, thus decreasing its mixing ratio and increasing the discrepancies between observation
25 and simulation. This is illustrated in Fig. 5 where we show a comparison of simulated values taken from S1 and this work with observations, taken from the PEM-Tropics-A campaign (Hoell et al., 1999). While simulation S1 is partially in agreement with the observations, simulations SR1 and SR2 show a substantial decrease in the acetic acid

Does acetone react with HO₂ in the upper-troposphere?

T. J. Dillon et al.

[Title Page](#)[Abstract](#)[Introduction](#)[Conclusions](#)[References](#)[Tables](#)[Figures](#)[⏪](#)[⏩](#)[◀](#)[▶](#)[Back](#)[Close](#)[Full Screen / Esc](#)[Printer-friendly Version](#)[Interactive Discussion](#)

mixing ratios ubiquitously in the troposphere. At the same time, in Fig. 5, no difference is noticeable between model results from simulation SR1 and SR2, showing that no significant amounts of acetic acid are formed in reaction (R1). The simulated rates of formation of acetic acid will depend critically on the model levels of NO_x and organic precursors for the acetylperoxy ($\text{CH}_3\text{C}(\text{O})\text{O}_2$) radical. Thus, the model output for NO, the levels of which determine whether $\text{CH}_3\text{C}(\text{O})\text{O}_2$ reacts with NO or with HO_2 to form $\text{CH}_3\text{C}(\text{O})\text{OH}$, were compared with measurements in the same region. Likewise, PAN, formed from combination of $\text{CH}_3\text{C}(\text{O})\text{O}_2$ with NO_2 may be considered an indicator of rates of $\text{CH}_3\text{C}(\text{O})\text{O}_2$ formation and a comparison between observation and model was also conducted. In both cases, the model was able to reproduce the observed levels of NO and PAN reasonably well, suggesting no important omissions in the model code in this regard. Exemplary plots are provided in the supplementary electronic information to illustrate this. Given that the kinetic database on the acetic acid sink via reaction with OH is now in good shape, the model-observation discrepancy is most likely due to missing source terms. Whilst noting that reaction between acetone and HO_2 clearly cannot contribute to significant acetic acid formation in the troposphere, further discussion of the atmospheric chemistry of acetic acid is beyond the scope of this study, which has ruled out a potential role of the title reaction.

4 Conclusions

The reaction $\text{HO}_2 + \text{CH}_3\text{C}(\text{O})\text{CH}_3 \rightleftharpoons (\text{CH}_3)_2\text{C}(\text{OH})\text{OO}$ (R1, R-1) was, for the first time, experimentally investigated in low-temperature conditions representative of the upper-troposphere. Evidence of reaction was observed in the lowest temperature experiments, allowing a lower limiting value of $k_1(207\text{ K}) \approx 1.6 \times 10^{-12} \text{ cm}^3 \text{ molecule}^{-1} \text{ s}^{-1}$ to be estimated, in line with theoretical predictions in line with the theoretical predictions of Hermans et al. (2004). At temperatures above 230 K there was no observable interaction, most likely due to rapid dissociation of the peroxy radical product back to reactants. An overall upper-limit to $K_1(T)$ of $7.8 \times 10^{-28} \exp\{50.6 \text{ kJ mol}^{-1} / (RT)\} \text{ cm}^3 \text{ molecule}^{-1}$

Does acetone react with HO_2 in the upper-troposphere?

T. J. Dillon et al.

Title Page

Abstract

Introduction

Conclusions

References

Tables

Figures

◀

▶

◀

▶

Back

Close

Full Screen / Esc

Printer-friendly Version

Interactive Discussion



was calculated from the results of this work. Incorporation of these results into a photochemical model of the atmosphere demonstrated that (R1) plays an insignificant role in either $\text{CH}_3\text{C}(\text{O})\text{CH}_3$ removal, or as a source of $\text{CH}_3\text{C}(\text{O})\text{OH}$.

Supplementary material related to this article is available online at:

<http://www.atmos-chem-phys-discuss.net/10/16747/2010/acpd-10-16747-2010-supplement.pdf>

Acknowledgements. This work was conducted as part of the EU integrated project SCOUT-O₃. AP thanks the International Max-Planck Research School for support.

The service charges for this open access publication have been covered by the Max Planck Society.

References

Arnold, F., Knop, G., and Ziereis, H.: Acetone measurements in the upper troposphere and lower stratosphere – implications for hydroxyl radical abundances, *Nature*, 321, 505–507, 1986.

Arnold, S. R., Chipperfield, M. P., and Blitz, M. A.: A three-dimensional model study of the effect of new temperature-dependent quantum yields for acetone photolysis, *J. Geophys. Res.-Atmos.*, 110, D22305, doi:10.1029/2005JD005998, 2005.

Atkinson, R. and Arey, J.: Atmospheric degradation of volatile organic compounds, *Chem. Rev.*, 103, 4605–4638, 2003.

Atkinson, R., Baulch, D. L., Cox, R. A., Crowley, J. N., Hampson, R. F., Hynes, R. G., Jenkin, M. E., Rossi, M. J., and Troe, J.: Evaluated kinetic and photochemical data for atmospheric chemistry: Volume I – gas phase reactions of O_x, HO_x, NO_x and SO_x species, *Atmos. Chem. Phys.*, 4, 1461–1738, doi:10.5194/acp-4-1461-2004, 2004.

Atkinson, R., Baulch, D. L., Cox, R. A., Crowley, J. N., Hampson, R. F., Hynes, R. G., Jenkin, M. E., Rossi, M. J., Troe, J., and IUPAC Subcommittee: Evaluated kinetic and photochemical data for atmospheric chemistry: Volume II – gas phase reactions of organic species, *Atmos. Chem. Phys.*, 6, 3625–4055, doi:10.5194/acp-6-3625-2006, 2006.

16762

ACPD

10, 16747–16773, 2010

Does acetone react with HO₂ in the upper-troposphere?

T. J. Dillon et al.

Title Page

Abstract

Introduction

Conclusions

References

Tables

Figures

⏪

⏩

◀

▶

Back

Close

Full Screen / Esc

Printer-friendly Version

Interactive Discussion



Does acetone react with HO₂ in the upper-troposphere?

T. J. Dillon et al.

Title Page

Abstract

Introduction

Conclusions

References

Tables

Figures

◀

▶

◀

▶

Back

Close

Full Screen / Esc

Printer-friendly Version

Interactive Discussion



- Benson, S. W.: Some observations on the kinetics and thermochemistry of the reactions of HO₂ radicals with aldehydes and ketones, *Int. J. Chem. Kinet.*, 33, 509–512, 2001.
- Cours, T., Canneaux, S., and Bohr, F.: Features of the potential energy surface for the reaction of HO₂ radical with acetone, *Int. J. Quantum Chem.*, 107, 1344–1354, 2007.
- 5 Curtis, A. R. and Sweetenham, W. P.: Facsimile, AERE, Report R-12805, 1987.
- Dillon, T. J. and Crowley, J. N.: Direct detection of OH formation in the reactions of HO₂ with CH₃C(O)O₂ and other substituted peroxy radicals, *Atmos. Chem. Phys.*, 8, 4877–4889, doi:10.5194/acp-8-4877-2008, 2008.
- Dillon, T. J., Hölscher, D., Sivakumaran, V., Horowitz, A., and Crowley, J. N.: Kinetics of the re-
actions of HO with methanol (210–351 K) and with ethanol (216–368 K), *Phys. Chem. Chem. Phys.*, 7, 349–355, 2005.
- 10 Dillon, T. J., Horowitz, A., Hölscher, D., and Crowley, J. N.: Reaction of HO with hydroxyacetone (HOCH₂C(O)CH₃): rate coefficients and mechanism., *Phys. Chem. Chem. Phys.*, 8, 236–246, 2006.
- 15 Gierczak, T., Burkholder, J. B., Bauerle, S., and Ravishankara, A. R.: Photochemistry of acetone under tropospheric conditions, *Chem. Phys.*, 231, 229–244, 1998.
- Gierczak, T., Gilles, M. K., Bauerle, S., and Ravishankara, A. R.: Reaction of hydroxyl radical with acetone, 1. Kinetics of the reactions of OH, OD, and (OH)-O-18 with acetone and acetone-d(6), *J. Phys. Chem. A*, 107, 5014–5020, 2003.
- 20 Gierczak, T. and Ravishankara, A. R.: Does the HO₂ radical react with ketones?, *Int. J. Chem. Kinet.*, 32, 573–580, 2000.
- Hasson, A. S., Tyndall, G. S., and Orlando, J. J.: A product yield study of the reaction of HO₂ radicals with ethyl peroxy (C₂H₅O₂), acetyl peroxy (CH₃C(O)O₂), and acetyl peroxy (CH₃C(O)CH₂O₂) radicals, *J. Phys. Chem. A*, 108, 5979–5989, 2004.
- 25 Hermans, I., Muller, J. F., Nguyen, T. L., Jacobs, P. A., and Peeters, J.: Kinetics of alpha-hydroxy-alkylperoxyl radicals in oxidation processes. HO₂ center dot-initiated oxidation of ketones/aldehydes near the tropopause, *J. Phys. Chem. A*, 109, 4303–4311, 2005.
- Hermans, I., Nguyen, T. L., Jacobs, P. A., and Peeters, J.: Tropopause chemistry revisited: HO₂*-initiated oxidation as an efficient acetone sink, *J. Am. Chem. Soc.*, 126, 9908–9909, 2004.
- 30 Hoell, J. M., Davis, D. D., Jacob, D. J., Rodgers, M. O., Newell, R. E., Fuelberg, H. E., McNeal, R. J., Raper, J. L., and Bendura, R. J.: Pacific exploratory mission in the tropical Pacific: PEM-Tropics A, August–September 1996, *J. Geophys. Res.-Atmos.*, 104, 5567–5583, 1999.

Does acetone react with HO₂ in the upper-troposphere?

T. J. Dillon et al.

Title Page

Abstract

Introduction

Conclusions

References

Tables

Figures

◀

▶

◀

▶

Back

Close

Full Screen / Esc

Printer-friendly Version

Interactive Discussion



IUPAC, subcommittee for gas kinetic data evaluation (Ammann, M., Atkinson, R., Cox, R. A., Crowley, J. N., Hynes, R. G., Jenkin, M. E., Mellouki, W., Rossi, M. J., Troe, J., and Wallington, T. J.): Evaluated kinetic data: <http://www.iupac-kinetic.ch.cam.ac.uk/>, 2010.

Jacob, D. J., Field, B. D., Jin, E. M., Bey, I., Li, Q., Logan, J. A., Yantosca, R. M., and Singh, H. B.: Atmospheric budget of acetone, *JGR*, 107, 5.1–5.17, 2002.

Jenkin, M. E., Hurley, M. D., and Wallington, T. J.: Investigation of the radical product channel of the $\text{CH}_3\text{C}(\text{O})\text{CH}_2\text{O}_2+\text{HO}_2$ reaction in the gas phase, *Phys. Chem. Chem. Phys.*, 10, 4274–4280, 2008.

Jeuken, A., Siegmund, P., Heijboer, L., Feichter, J., and Bengtsson, L.: On the potential assimilating meteorological analyses in a global model for the purpose of model validation, *J. Geophys. Res.*, 101(D12), 16939–16950, doi:10.1029/96JD01218, 1996

Jöckel, P., Sander, R., Kerkweg, A., Tost, H., and Lelieveld, J.: Technical Note: The Modular Earth Submodel System (MESSy) – a new approach towards Earth System Modeling, *Atmos. Chem. Phys.*, 5, 433–444, doi:10.5194/acp-5-433-2005, 2005.

Jöckel, P., Tost, H., Pozzer, A., Brühl, C., Buchholz, J., Ganzeveld, L., Hoor, P., Kerkweg, A., Lawrence, M. G., Sander, R., Steil, B., Stiller, G., Tanarhte, M., Taraborrelli, D., van Aardenne, J., and Lelieveld, J.: The atmospheric chemistry general circulation model ECHAM5/MESSy1: consistent simulation of ozone from the surface to the mesosphere, *Atmos. Chem. Phys.*, 6, 5067–5104, doi:10.5194/acp-6-5067-2006, 2006.

Lelieveld, J., Brühl, C., Jöckel, P., Steil, B., Crutzen, P. J., Fischer, H., Giorgetta, M. A., Hoor, P., Lawrence, M. G., Sausen, R., and Tost, H.: Stratospheric dryness: model simulations and satellite observations, *Atmos. Chem. Phys.*, 7, 1313–1332, doi:10.5194/acp-7-1313-2007, 2007.

Maricq, M. M. and Szente, J. J.: The UV spectrum of acetyl and the kinetics of the chain reaction between acetaldehyde and chlorine, *Chem. Phys. Lett.*, 253, 333–339, 1996.

McKeen, S. A., Gierzak, T., Burkholder, J. B., Wennberg, P. O., Hanisco, T. F., Keim, E. R., Gao, R.-S., Liu, S. C., Ravishankara, A. R., and Fahey, D. W.: The photochemistry of acetone in the upper troposphere: a source of odd-hydrogen radicals, *Geophys. Res. Lett.*, 24, 3177–3180, 1997.

Nesbitt, F. L., Payne, W. A., and Stief, L. J.: Temperature-Dependence for the absolute rate-constant for the reaction $\text{CH}_2\text{OH}+\text{O}_2\rightarrow\text{HO}_2+\text{H}_2\text{CO}$ from 215 K to 300 K, *J. Phys. Chem.*, 92, 4030–4032, 1988.

Does acetone react with HO₂ in the upper-troposphere?

T. J. Dillon et al.

[Title Page](#)[Abstract](#)[Introduction](#)[Conclusions](#)[References](#)[Tables](#)[Figures](#)[◀](#)[▶](#)[◀](#)[▶](#)[Back](#)[Close](#)[Full Screen / Esc](#)[Printer-friendly Version](#)[Interactive Discussion](#)

- Pozzer, A., Jöckel, P., Tost, H., Sander, R., Ganzeveld, L., Kerkweg, A., and Lelieveld, J.: Simulating organic species with the global atmospheric chemistry general circulation model ECHAM5/MESSy1: a comparison of model results with observations, *Atmos. Chem. Phys.*, 7, 2527–2550, doi:10.5194/acp-7-2527-2007, 2007.
- 5 Sander, R., Kerkweg, A., Jöckel, P., and Lelieveld, J.: Technical note: The new comprehensive atmospheric chemistry module MECCA, *Atmos. Chem. Phys.*, 5, 445–450, doi:10.5194/acp-5-445-2005, 2005.
- Singh, H. B., Kanakidou, M., Crutzen, P. J., and Jacob, D. J.: High concentrations and photochemical fate of oxygenated hydrocarbons in the global troposphere, *Nature*, 378, 50–54, 1995.
- 10 Timonen, R.: Kinetics of the reactions of some polyatomic free radicals with Cl₂ and Br₂, and reactions of formyl radicals with O₂, NO₂, Cl₂, Br₂, and H atoms, *Ann. Acad. Sci. Fenn. Ser. A2*, 218, 5–45, 1988.
- Tomas, A., Villenave, E., and Lesclaux, R.: Reactions of the HO₂ radical with CH₃CHO and CH₃C(O)O₂ in the gas phase, *J. Phys. Chem. A*, 105, 3505–3514, 2001.
- 15 Veyret, B., Lesclaux, R., Rayez, M.-T., Rayez, J.-C., Cox, R. A., and Moortgat, G. K.: Kinetics and mechanism of the photooxidation of formaldehyde, 1. Flash photolysis study, *J. Phys. Chem.*, 93, 2368–2374, 1989.
- Wennberg, P. O., Hanisco, T. F., Jaeglé, L., Jacob, D. J., Hintsä, E. J., Lanzendorf, E. J., Anderson, J. G., Gao, R.-S., Keim, E. R., Donnelly, S. G., Del Negro, L. A., Fahey, D. W., McKeen, S. A., Salawitch, R. J., Webster, C. R., May, R. D., Herman, R. L., Proffitt, M. H., Margitan, J. J., Atlas, E. L., Schauffler, S. M., Flocke, F., McElroy, C. T., and Bui, T. P.: Hydrogen radicals, nitrogen radicals, and the production of O₃ in the upper troposphere, *Science*, 279, 49–53, 1998.
- 20 Wollenhaupt, M., Carl, S. A., Horowitz, A., and Crowley, J. N.: Rate coefficients for reaction of OH with acetone between 202 and 395 K, *J. Phys. Chem.*, 104, 2695–2705, 2000.
- 25

Does acetone react with HO₂ in the upper-troposphere?

T. J. Dillon et al.

[Title Page](#)
[Abstract](#)
[Introduction](#)
[Conclusions](#)
[References](#)
[Tables](#)
[Figures](#)
[Back](#)
[Close](#)
[Full Screen / Esc](#)
[Printer-friendly Version](#)
[Interactive Discussion](#)


Table 1. Modifications to the chemical scheme used in the modelling studies.

Reaction	k^a
$\text{HO}_2 + \text{CH}_3\text{C}(\text{O})\text{CH}_3 \rightarrow (\text{CH}_3)_2\text{C}(\text{OH})\text{OO}$	$5.1 \times 10^{-15} \exp(1335/T)$
$(\text{CH}_3)_2\text{C}(\text{OH})\text{OO} \rightarrow \text{HO}_2 + \text{CH}_3\text{C}(\text{O})\text{CH}_3$	$6.5 \times 10^{12} \exp(-4750/T) \text{ s}^{-1}$
$(\text{CH}_3)_2\text{C}(\text{OH})\text{OO} + \text{NO} \rightarrow \text{CH}_3\text{O}_2 + \text{CH}_3\text{C}(\text{O})\text{OH} + \text{NO}_2$	$2.7 \times 10^{-12} \exp(360/T)$
$(\text{CH}_3)_2\text{C}(\text{OH})\text{OO} + \text{HO}_2 \rightarrow (\text{CH}_3)_2\text{C}(\text{OH})\text{OOH} + \text{O}_2$	4×10^{-11}
$\text{CH}_3\text{C}(\text{O})\text{OH} + \text{OH} \rightarrow \text{CH}_3\text{O}_2$	$4.0 \times 10^{-14} \exp(850/T)$
$\text{CH}_3\text{C}(\text{O})\text{O}_2 + \text{HO}_2 \rightarrow \text{CH}_3\text{C}(\text{O})\text{O}_2\text{H}$	$0.41 \times 5.2 \times 10^{-13} \exp(980/T)$
$\text{CH}_3\text{C}(\text{O})\text{O}_2 + \text{HO}_2 \rightarrow \text{CH}_3\text{C}(\text{O})\text{OH}$	$0.15 \times 5.2 \times 10^{-13} \exp(980/T)$
$\text{CH}_3\text{C}(\text{O})\text{O}_2 + \text{HO}_2 \rightarrow \text{CH}_3\text{O}_2 + \text{OH}$	$0.44 \times 5.2 \times 10^{-13} \exp(980/T)$
$\text{CH}_3\text{C}(\text{O})\text{O}_2 + \text{CH}_3\text{O}_2 \rightarrow \text{HCHO} + \text{HO}_2 + \text{CH}_3\text{O}_2$	$0.9 \times 2 \times 10^{-12} \exp(500/T)$
$\text{CH}_3\text{C}(\text{O})\text{O}_2 + \text{CH}_3\text{O}_2 \rightarrow \text{CH}_3\text{C}(\text{O})\text{OH} + \text{HCHO}$	$0.1 \times 2 \times 10^{-12} \exp(500/T)$
$\text{CH}_3\text{C}(\text{O})\text{O}_2 + \text{C}_2\text{H}_5\text{O}_2 \rightarrow 0.82\text{CH}_3\text{O}_2 + \text{CH}_3\text{CHO} + 0.82\text{HO}_2 + 0.18\text{CH}_3\text{C}(\text{O})\text{OH}$	$4.4 \times 10^{-13} \exp(1070/T)$

^a k in units of $\text{cm}^3 \text{ molecule}^{-1} \text{ s}^{-1}$ unless stated otherwise.

Does acetone react with HO₂ in the upper-troposphere?

T. J. Dillon et al.

Table 2. Experimental conditions and determinations of $K_1(T)$.

T/K	P/Torr	$[\text{CH}_3\text{OH}]^a$	$[\text{NO}]^a$	$[\text{O}_2]^a$	$[\text{CH}_3\text{C}(\text{O})\text{CH}_3]^a$	n^b	k_1^c	K_1
207	25	4.7	1.5	440	0–7.5	7	1.6	14.0
210	25	4.6	1.5	430	0–7.4	8	1.1	6.5
215	25	4.5	1.4	420	0–7.1	6	0.5	4.6
220	85	8.2	1.4	570	0–16.2	5	0.3	1.5
228	85	10.0	2.4	530	0–17.2	6	~0.1	0.6
235	85	16	2.6	900	0–14.5	5	n/a	n/a
273	85	17	3.3	450	0–12.4	6	n/a	n/a
298	85	16	3.0	410	0–11.3	6	n/a	n/a

^a all reagent concentrations in units of 10^{14} molecule cm^{-3} ;

^b n = number of experiments at different $[\text{CH}_3\text{C}(\text{O})\text{CH}_3]$;

^c lower limits to $k_1/10^{-12}$ cm^3 molecule⁻¹ s⁻¹ calculated assuming $k_{-1}=0$; K_1 in units of 10^{-16} cm^3 molecule⁻¹.

Title Page

Abstract

Introduction

Conclusions

References

Tables

Figures

◀

▶

◀

▶

Back

Close

Full Screen / Esc

Printer-friendly Version

Interactive Discussion



Does acetone react with HO₂ in the upper-troposphere?

T. J. Dillon et al.

Title Page

Abstract

Introduction

Conclusions

References

Tables

Figures

◀

▶

◀

▶

Back

Close

Full Screen / Esc

Printer-friendly Version

Interactive Discussion



Table 3. Chemistry used in numerical simulations (Sect. 3).

Reaction	k^a	Ref. ^b
Cl+CH ₃ OH→CH ₂ OH+HCl	$1.4 \times 10^{-10} \exp(-280/T)$	
Cl+CH ₃ C(O)CH ₃ →CH ₂ C(O)CH ₃ +HCl	$1.5 \times 10^{-11} \exp(-590/T)$	
CH ₂ OH+O ₂ →HCHO+HO ₂	$5.6 \times 10^{-9} \exp(-1700/T)$	Nesbitt et al. (1988)
CH ₂ OH+Cl ₂ →Cl+ClCH ₂ OH	2.7×10^{-11}	
NO+HO ₂ →OH+NO ₂	$3.6 \times 10^{-12} \exp(270/T)$	
HO ₂ +HO ₂ →H ₂ O ₂ +O ₂	$2.2 \times 10^{-13} \exp(600/T) + 1.9 \times 10^{33} [M] \exp(980/T)$	
HO ₂ +CH ₃ C(O)CH ₃ →(CH ₃) ₂ C(OH)OO	varied	
(CH ₃) ₂ C(OH)OO→HO ₂ +CH ₃ C(O)CH ₃	varied	
OH+CH ₃ OH→CH ₂ OH+H ₂ O	$0.85 \times 6.67 \times 10^{-18} T^2 \exp[(140)/T]$	Dillon et al. (2005)
OH+CH ₃ OH→CH ₃ O+H ₂ O	$0.15 \times 6.67 \times 10^{-18} T^2 \exp(140/T)$	Dillon et al. (2005)
OH+CH ₃ C(O)CH ₃ →CH ₂ C(O)CH ₃ +H ₂ O	$8.8 \times 10^{-12} \exp(-1320/T) + 1.7 \times 10^{-14} \exp(423/T)$	
OH+NO+M→HONO+M	$k_0 = 7.4 \times 10^{-31} (T/300)^{-2.4} [N_2]$, $k_\infty = 3.3 \times 10^{-11} (T/300)^{-0.3}$, $F_c = 0.81$	
(CH ₃) ₂ C(OH)OO+NO→CH ₃ +CH ₃ C(O)OH+NO ₂	$2.7 \times 10^{-12} \exp(360/T)$	estimate, see text
(CH ₃) ₂ C(OH)OO+HO ₂ →(CH ₃) ₂ C(OH)OOH+O ₂	4×10^{-11}	estimate
CH ₂ C(O)CH ₃ +O ₂ →O ₂ CH ₂ C(O)CH ₃	$7.2 \times 10^{-13} \exp(130/T)$	
O ₂ CH ₂ C(O)CH ₃ +NO→OCH ₂ C(O)CH ₃	$2.8 \times 10^{-12} \exp(300/T)$	
OCH ₂ C(O)CH ₃ +O ₂ →CH ₃ CO	1.0×10^{-13}	estimate
CH ₃ CO+O ₂ →CH ₃ C(O)O ₂	5.1×10^{-12}	
CH ₃ CO+Cl ₂ →CH ₃ C(O)Cl+Cl	$2.8 \times 10^{-11} \exp(-47/T)$	Maricq and Szente (1996)
CH ₃ C(O)O ₂ +NO→CH ₃ +CO ₂ +NO ₂	$7.5 \times 10^{-12} \exp(290/T)$	
CH ₃ +O ₂ +M→CH ₃ O ₂ +M	$1 \times 10^{-30} (T/300)^{-3.3} [N_2]$	
CH ₃ +Cl ₂ →CH ₃ Cl+Cl	$4.79 \times 10^{-12} \exp(-240/T)$	Timonen (1988)
CH ₃ O ₂ +NO→CH ₃ O+NO ₂	$2.3 \times 10^{-12} \exp(360/T)$	
CH ₃ O+O ₂ →HO ₂ +HCHO	1.9×10^{-15}	
CH ₃ O+NO→HNO+HCHO	$2.3 \times 10^{-12} (T/300)^{-0.7}$	
CH ₃ O+NO+M→CH ₃ ONO+M	$2.6 \times 10^{-29} (T/300)^{-2.8} [M]$	

^a k in units of cm³ molecule⁻¹ s⁻¹ unless stated otherwise;

^b values taken from (IUPAC, 2010) unless stated otherwise.

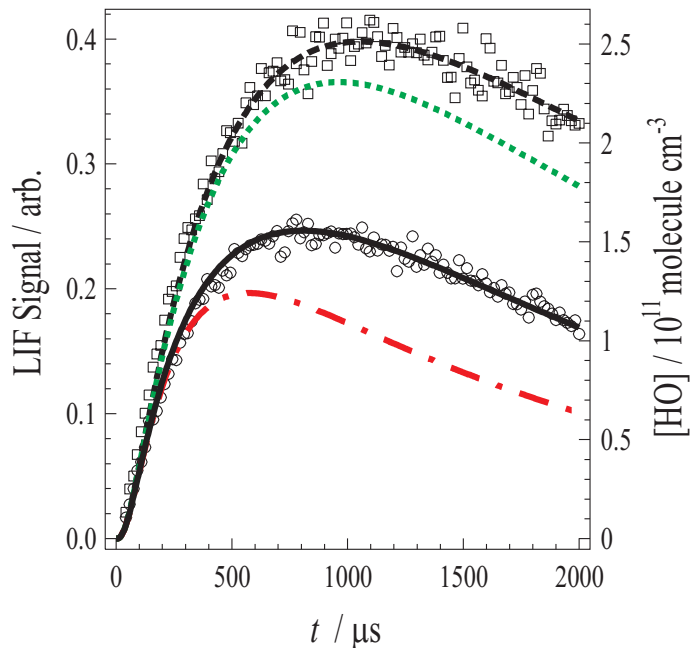


Fig. 1. OH LIF profiles recorded following HO_2 generation (R5–R7) in the presence of NO ($1.5 \times 10^{14} \text{ molecule cm}^{-3}$) at 207 K and 25 Torr. Squares are data with $[\text{CH}_3\text{C}(\text{O})\text{CH}_3]=0$. The black dashed line is the numerical simulation used to calibrate the LIF signal response. Circles are datapoints with $[\text{CH}_3\text{C}(\text{O})\text{CH}_3]=7.5 \times 10^{14} \text{ molecule cm}^{-3}$, and are associated with 3 numerical simulations. The solid black line was generated using $k_1=5.1 \times 10^{-15} \exp(11100/RT) \text{ cm}^3 \text{ molecule}^{-1} \text{ s}^{-1}$ in conjunction with a value of $k_{-1}=2300 \text{ s}^{-1}$. Results from simulations using theoretical values of k_1 and k_{-1} are depicted as the red dash-dotted (Hermans et al., 2004) and the green dotted line (Cours et al., 2007).

Does acetone react with HO_2 in the upper-troposphere?

T. J. Dillon et al.

Title Page	
Abstract	Introduction
Conclusions	References
Tables	Figures
◀	▶
◀	▶
Back	Close
Full Screen / Esc	
Printer-friendly Version	
Interactive Discussion	



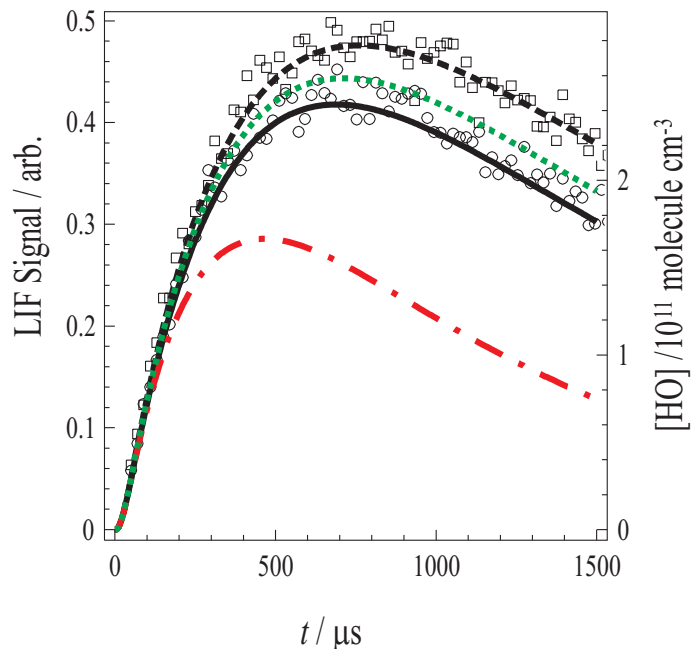


Fig. 2. OH LIF profiles recorded following HO_2 generation in the presence of NO ($1.6 \times 10^{14} \text{ molecule cm}^{-3}$) at 228 K and 85 Torr. Squares datapoints were obtained with $[\text{CH}_3\text{C(O)CH}_3]=0$ and the black dashed line is the associated numerical simulation used to calibrate the LIF signal response. Circles are data obtained at $[\text{CH}_3\text{C(O)CH}_3]=1.0 \times 10^{15} \text{ molecule cm}^{-3}$ and are associated with 3 numerical simulations: The solid black line generated using $k_1=5.1 \times 10^{-15} \exp(11100/RT) \text{ cm}^3 \text{ molecule}^{-1} \text{ s}^{-1}$ and $k_{-1}=30000 \text{ s}^{-1}$. Results from simulations using theoretical values of k_1 and k_{-1} from Hermans et al. are depicted as the red dot-dashed line. The green dotted line represents $k_1=0$ (indistinguishable from simulations using parameters from Cours et al., 2007).

Does acetone react with HO_2 in the upper-troposphere?

T. J. Dillon et al.

Title Page	
Abstract	Introduction
Conclusions	References
Tables	Figures
◀	▶
◀	▶
Back	Close
Full Screen / Esc	
Printer-friendly Version	
Interactive Discussion	



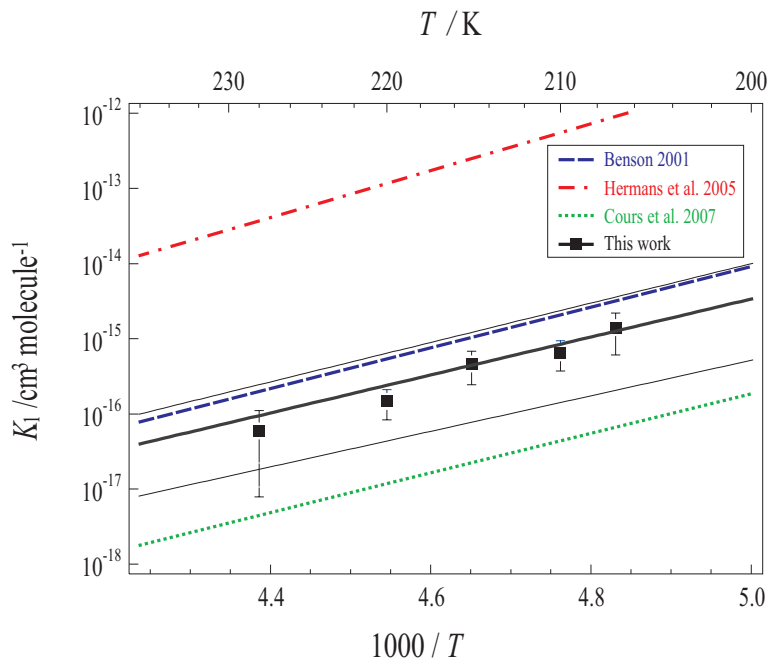


Fig. 3. Van't Hoff plot used to compare determinations of K_1 . The dashed blue line represents an extrapolation from the $K_1(298 \text{ K})$ value estimated by Benson (2001). The red dot-dashed line and green dotted lines depict the results from, respectively Hermans et al. (2004) and Cours et al. (2007). The square datapoints depict values of K_1 obtained in this work; with error bars representative of experimental scatter. The solid black line depicts a "3rd Law" fit to the data, with the pre-exponential factor fixed to the calculated reaction entropy (Hermans et al., 2004) to yield $K_1(T) = 7.8 \times 10^{-28} \exp\{(48.4 \pm 0.3) \text{ kJ mol}^{-1} / RT\} \text{ cm}^3 \text{ molecule}^{-1}$; the corresponding hairlines represent estimates of overall systematic uncertainty (see text for details).

Does acetone react with HO₂ in the upper-troposphere?

T. J. Dillon et al.

Title Page

Abstract

Introduction

Conclusions

References

Tables

Figures

◀

▶

◀

▶

Back

Close

Full Screen / Esc

Printer-friendly Version

Interactive Discussion



Does acetone react with HO₂ in the upper-troposphere?

T. J. Dillon et al.

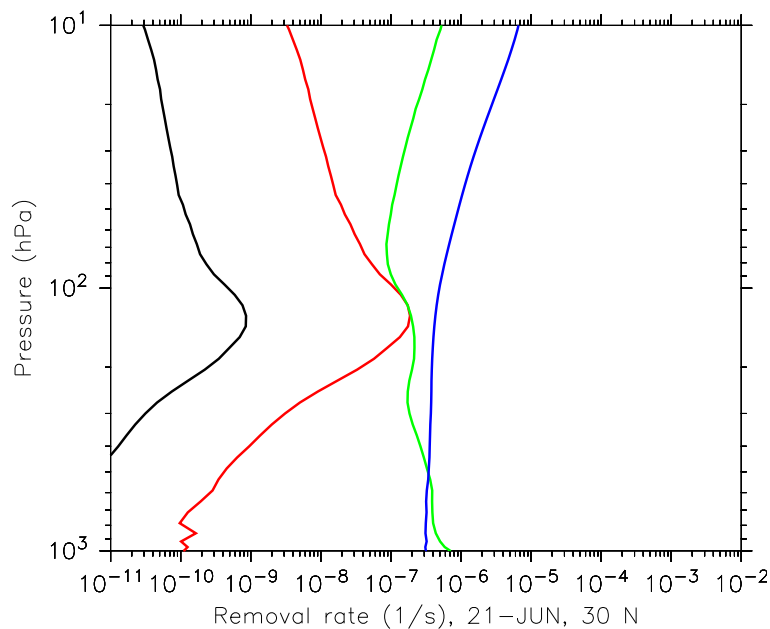


Fig. 4. CH₃C(O)CH₃ removal rates at 30° N solstice initiated by: photolysis (R3) in blue; reaction with OH (R4) in green; and the reaction of interest (R1) using parameters from (Hermans et al., 2004) (in red) and those derived in this work (black).

[Title Page](#)[Abstract](#)[Introduction](#)[Conclusions](#)[References](#)[Tables](#)[Figures](#)[◀](#)[▶](#)[◀](#)[▶](#)[Back](#)[Close](#)[Full Screen / Esc](#)[Printer-friendly Version](#)[Interactive Discussion](#)

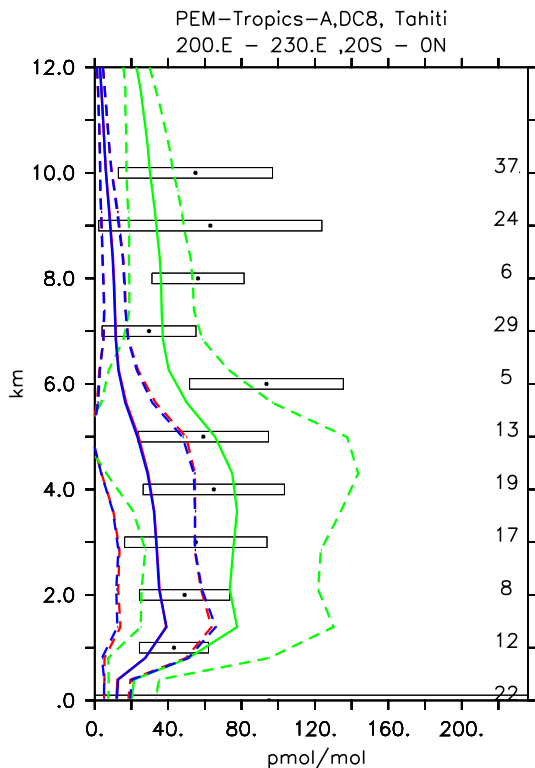


Fig. 5. Vertical profiles of $\text{CH}_3\text{C}(\text{O})\text{OH}$ (nmol/mol) from simulations and observations. Asterisks and boxes represent the average and the standard deviation (with respect to space and time) of the measurements from a specific region (Tahiti) taken during the PEM-Tropics-A campaign. On the right side the number of measurements for the specific region is listed. The simulated average is indicated by the line and the corresponding standard deviation with respect to time and space by the dashed lines. The blue, red and green lines represents model results from simulations SR1, SR2 and S1, respectively.

Does acetone react with HO_2 in the upper-troposphere?

T. J. Dillon et al.

Title Page

Abstract

Introduction

Conclusions

References

Tables

Figures

◀

▶

◀

▶

Back

Close

Full Screen / Esc

Printer-friendly Version

Interactive Discussion

